J. At. Mol. Sci.
doi: 10.4208/jams.031112.042312a

Vol. **4** , No. 1 , pp. 64-71
February 2013

24R-type LPSO microstructure of the novel Mg-Y-Zn alloy

Yong-He Deng*

College of Science, Hunan Institute of Engineering, Xiangtan 411104, China

Received 11 March 2012; Accepted (in revised version) 23 April 2012
Published Online 8 December 2012

Abstract. The microstructue of the novel long period stacking ordered(LPSO) structure in Mg-Y-Zn alloy has been systematically studied based on the density functional theory. The lattice positions of the Y and Zn atoms are determined theoretically, it is shown that the additive atoms are firstly enriched in the stacking fault layers at the two ends, a small amount are distributed in the interior stacking fault layers of the structure. And the arrangement of these Y and Zn atoms trends to be along the diagonal line of the unit cell.

PACS: 61.50.Ah, 63.20.dk, 81.05.Bx

Key words: Mg-Y-Zn alloy, LPSO, additive atoms, density functional theory, microstructure

1 Introduction

Mg-based alloys have become more and more important nowdays, because of its low density, high specific strength and elastic modulus and high recycling efficiency [1]. Mg-based alloys with excellent properties have been applied in many fields such as microelectronics, automobile and aerospace industries. To further improve the mechanical properties of Mg-based alloys, great endeavor has been made through adding rare-earth (RE) elements and transition metal elements. Recently, superior performance of Mg-Y-Zn alloy with extremely high tensile yield strength of 610MPa and elongation of 5% has been recently developed by rapidly solidified (RS) powder metallurgy [2-5]. Furthermore, the Mg-Y-Zn alloy still shows high corrosion resistance at room temperature [6].

The excellent properties of Mg-Y-Zn alloy are due to the hcp (2H)-Mg fine grain matrix of 100-200 nm with a novel long-period stacking ordered (LPSO) phase and homogeneously dispersed $Mg_{24}Y_5$ fine particles of less than 10 nm [7-9]. The morphological, crystallographic and chemical characterizations of the LPSO phase have been performed

*Corresponding author. *Email address:* dengyonghe@163.com (Y. -H. Deng)

 © 2013 Global-Science Press

by conventional transmission electron microscope (CTEM) [7], high-angle annular dark-field scanning TEM with Z-contrast [8], high-resolution transmission electron microscope (HRTEM) observations [10], and three-dimensional atom probe [11]. So far, five kinds of LPSO structures (6H, 10H, 14H, 18R, and 24R) are observed in these Mg-based alloys [7]. The 6H, 14H and 18R structures are dominantly observed while the 10H and 24R are relatively rare. The novel LPSO structures have also been observed in other Mg-RE-Zn alloys and Mg-RE-Cu alloys [11-14]. Due to its importance in improving the mechanical properties of the Mg-based alloys, investigation of the structure and properties of the novel LPSO is crucial for design and application of the alloy materials.

2 Computation details

The present work is based on density functional theory at the level of the generalized gradient approximation (GGA) (using the PW-91 exchange-correlation functional). The method was implemented in the Vienna Ab initio Simulation Package (VASP) program, which used a plane-wave basis set with a kinetic energy cutoff at 300 eV and ultra-soft pseudopotentials for the election-ion interaction, the valence electron configurations considered are 3*s*, 2*p* for Mg, 3*d*, 4*s* for Zn and 4*s*, 4*p*, 5*s*, 4*d* for Y. For the 24R-type (ABABABABCACACACABCBCBCBC) LPSO structure in Mg-Y-Zn alloy, the supercell with 96 atoms (2×2 unit cell of 24 layers) is adopted. The Brillouin zone (BZ) is sampled with a mesh of $8\times8\times1$ k-points of Monkhorst-Pack scheme for 2×2 unit cell of 24 layers as supercell of 24R-type LPSO structure. And $10\times10\times1$ is chose for the electronic density of states. The convergence tests with respect to these parameters show that the error bar for the total energy is less than 1meV/atom ($\approx$0.1kJ/mol) [15]. These parameters have been tested to be sufficient for convergence. Structural optimization is performed using the first-order Methfessel-Paxton method with a temperature broadening parameter of 0.2 eV, and the positions of atoms are fully relaxed until the total forces on each ion are less than 0.02 eV/Å. Ionic relaxation and electronic energy minimization were performed using the conjugate gradient (CG) algorithm. For the calculation for density of states (DOS), the tetrahedron method with Bloch corrections were used as implemented in VASP.

3 Results and discussion

3.1 The microstructure

The lattice constants of pure Mg, Y and Zn are calculated to test the calculation parameters and pseudopotentials. The obtained results for pure Mg is $a=0.320$ nm and $c=0.513$ nm, for Y $a=0.365$ nm and $c=0.567$ nm, for Zn $a=2.67$ nm and $c=0.484$ nm, respectively. These results are agreement well with experimental values and other theoretical calculations [16]. So the present calculation results are reasonable and reliable.

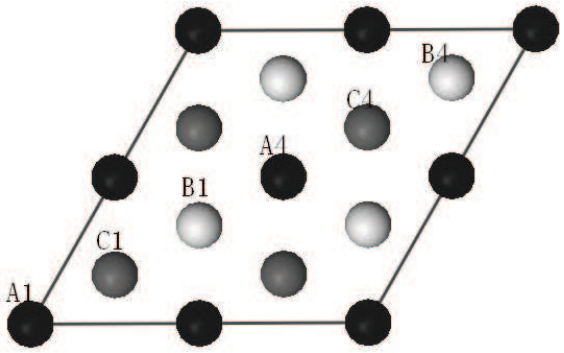

Figure 1: The atomic arrangement model of Mg-Y-Zn LPSO phase with 2×2 unit cell, and A1, B1 and C1 represent the layer of A, B and C, respectively.

Table 1: The total energies with Y and Zn atoms in the 24R-type LPSO.

Layer	A	BAB ABA	B	C	ACAC AC	A	B	CBC BCB	C	E(eV)
1	Y									-150.98777
2			Y							-150.92620
3				Y						-150.92392
4						Y				-150.92723
5							Y			-150.92702
6									Y	-150.92712
7	Zn									-145.58270
8			Zn							-145.57855
9				Zn						-145.58113
10						Zn				-145.58254
11							Zn			-145.58222
12									Zn	-145.57944

To describe suitably the positions of the additive atoms and the arrangement rule, and further to reveal the evolution of the microstructure of 24R-type LPSO phase with the concentration of Y and Zn elements, the two-dimensional lattice of 2×2 unit cell in the basal plane of the structure is shown in Fig.1. When only one Y or Zn atom is in the LPSO phase, the calculations in the Table 1 show that Y or Zn would be located in the first A layer at the end of the LPSO phase. Considering the fact that the ratio of Y to Zn is about 2:1 in the LPSO structure, and partial enthalpy of Mg-Y -27kJ/mol [17] is smaller than -4.1kJ/mol of Mg-Zn [18], The Y atom is assumed first to occupy the origin of the first layer in the unit cell, labeled by point A1 in Fig. 1. Then another Y or Zn is continuously added. From the calculated results in the Table 2, the followed Zn atom would be located in the A4 position in the same layer. Whereas the calculated results in

Table 2: The total energies with 1Y + 1Zn and 2Y atoms in the 24R-type LPSO.

Layer	A	BABA BA	B	C	ACA CAC	A	B	CBCB CB	C	E(eV)
1	Y+Zn									-150.69589
2	Y		Zn							-150.42534
3	Y			Zn						-150.54305
4	Y					Zn				-150.55045
5	Y						Zn			-150.55093
6	Y								Zn	-150.55062
7	2Y									-155.68380
8	Y		Y							-155.90601
9	Y			Y						-155.91249
10	Y					Y				-156.10760
11	Y						Y			-155.91121
12	Y								Y	-156.26761

Table 3: The total energies with 2Y+ 1Zn and 1Y+ 2Zn atoms in the 24R-type LPSO (x represents 1Y +1Zn).

Layer	A	BABA BA	B	C	ACAC AC	A	B	CBC BCB	C	E(eV)
1	x									-156.05660
2	x		Y							-155.67169
3	x			Y						-155.64345
4	x					Y				-155.65287
5	x						Y			-155.67479
6	x								Zn	-150.47618
7	x		Zn							-150.32860
8	x			Zn						-150.33176
9	x					Zn				-150.32928
10	x						Zn			-150.32192

Table 2 indicate that the second Y atom would diffuse to the position C4 in the C layer at the other end of the LPSO phase.

With further addition of the followed Y and Zn atoms, the calculated results are shown in Table 3. In the case of 2Y+1Zn, the arrangement configuration is naturally (A1+C4)+A4. For further addition of one more Zn atom, Table 4 shows that it is located in the position C1, corresponding to the arrangement configuration of (A1+A4)+(C4+C1) for 2Y+2Zn. Therefore, these atoms are firstly enriched in the two ends of the supercell. The investigation is well agreement with the experiment and the theoretic study [7]. It should be noticed that the Y and Zn atoms in the fault layers at the two ends of the structure would arrange in the opposite direction along the parallel diagonal line.

Table 4: The total energies with 2Y+ 2Zn atoms in the 24R-type LPSO (x represents 1Y +1Zn).

Layer	A	BABA BA	B	C	ACA CAC	A	B	CBC BCB	C	E(eV)
1	x								x	-155.96707
2	x		Zn						Y	-155.67658
3	x			Zn					Y	-155.67696
4	x					Zn			Y	-155.67663
5	x						Zn		Y	-155.67961

Table 5: The total energies with 3Y+ 2Zn and 2Y+ 3Zn atoms in the 24R-type LPSO (x represents 1Y+1Zn).

Layer	A	BABA BA	B	C	ACAC AC	A	B	CBC BCB	C	E(eV)
1	x		Y						x	-160.91194
2	x			Y					x	-160.93323
3	x					Y			x	-160.93031
4	x						Y		x	-160.93990
5	x		Zn						x	-155.60937
6	x			Zn					x	-155.80431
7	x					Zn			x	-155.60243
8	x						Zn		x	-155.59873

For the 2×2 unit cell in the basal plane layer, the saturation of substitution atom in each fault layer is approximately 2at.% for 24R-type LPSO structure. With further addition of Y and Zn atoms, the calculated results in Table 5 show that the followed Y and Zn atom are located in the position B1 in the 17th layer B and B4 in the 8th layer B, respectively, as it displays in the Fig. 1. Because the 8th and 17th layer B are the stacking fault layers, the present results show that these additive atoms are firstly enriched in the stacking fault layers at the two ends, then a small amount are distributed to the fault layers in the interior of the 24R-type LPSO phase. This distribution feature of additive atoms is in accordance with the experimental observation [9,19].

Because atomic radii of Y is larger than that of Mg whereas Zn is less than that of Mg, the influence of additive Y and Zn atoms on the lattice parameters is also investigated. Fig. 2 show that addition of Y into the fault Mg results in a small increase of lattice a and c as well as immediately adjacent interlayer spacing d_1. It should be noticed that the interlayer spacing d_n far away from the Y atom exhibits slight reduction. While addition of Zn into the fault Mg leads to decrease of a, d_n and c, but this reduction could be negligible. Moreover, simultaneous additive Y and Zn atoms, Zn atom could effectively offset the increase of a, d_1 and c resulting from Y atom. On the other hand, lattice distortion is an important feature of the LPSO structures in $Mg_{97}Zn_1Y_2$ alloy, it means that the c-axis is not perpendicular to the a-axis. Careful inspection on the shape of the unit cell, it is found

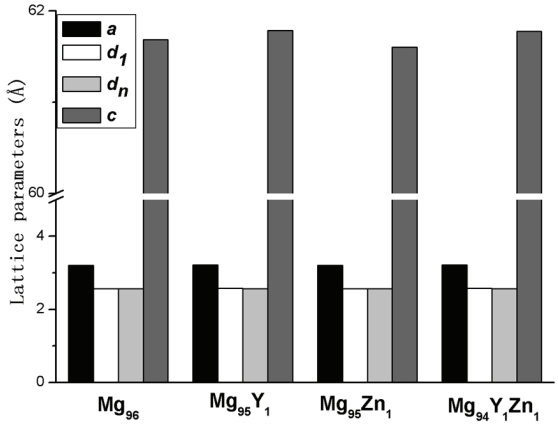

Figure 2: The lattice parameters a and c, the interlayer spacing of d_1 and d_n with different Y and Zn atoms in the 24R-type LPSO.

that the maximal angle between c-axis and the a-axis is about 89°. So the lattice distortion is very small. In our previous study on 6H and 10H LPSO structure, it is demonstrated that the lattice distortion occurs when Zn is dissymmetry in the LPSO phase.

3.2 Structural stability

Because five kinds of LPSO observed in these Mg-based alloys are similar in structure and could be transformed from each other, the stability of these LPSO phases is necessary. The phase stability is correlated to its cohesive energy [20], and the cohesive energy is often defined as energy needed when crystal is decomposed into the single atom. Hence, the lower the cohesive energy is, the more stable the crystal structure is [20]. In this work, average cohesive energy per atom for $Mg_{97}Zn_1Y_2$ ternary alloy was calculated using the following expression [21]

$$E_{coh} = \frac{1}{x+y+z}\left(E_{tot} - xE_{atom}^{Mg} - yE_{atom}^{y} - zE_{atom}^{Zn}\right)$$

where E_{tot} is the electronic total energy of unit cell of 24R-type LPSO, x, y and z also are the number of Mg, Y and Zn atoms in unit cell of 24R-type LPSO, E_{atom}^{Mg}, E_{atom}^{y} and E_{atom}^{Zn} are the electronic total energies of single Mg, Y and Zn atom in freedom states. They are -0.0398 eV, -1.9870 eV and -0.0055 eV for Mg, Y and Zn atoms, respectively. The calculated cohesive energies are displayed clearly in Fig. 3. It is found that when the Zn atoms are added the cohesive energies becoming slightly higher, whereas the additive Y atoms decrease obviously the cohesive energies. Consequently, the additive Y atoms would increase the phase stability from the energetic point of view. The underlying mechanism is determined by the electronic structure, as described in the following. Because the stability of intermetallics plays an important role in improving the creep property of

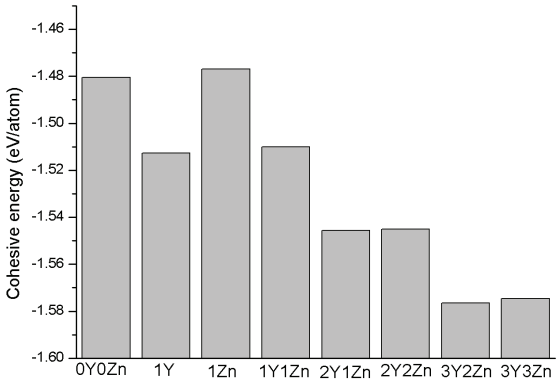

Figure 3: The cohesive energy (eV) of different Y and Zn atoms in the 24R-type LPSO.

magnesium alloys [22], the creep property of novel LPSO structure alloy would be improved by the high stability. Although Zn atom has not positive influence on the stability, it could bring about apparent improvement of mechanical properties such as ductility, as described in the following.

4 Conclusions

In the present work, first-principles calculations based on density functional theory have been carried out to study the microstructure of Mg-Y-Zn 24R-type LPSO phase. The lattice position and arrangement rule of the Y and Zn atoms are determined. The results show that the additive Y and Zn atoms are firstly enriched in the stacking fault layers at the two ends of the 24R-type LPSO, and a small amount are distributed in the stacking fault layers in the interior of the 24R-type LPSO.

Acknowledgments This work is supported by the Scientific Research Fund of Education Department of Hunan Province of China under Grant No. 09B021.

References

[1] R. L. Edgar, Magnesium Alloys and their Application (K.U. Kainer Pub, France, 2000).
[2] Y. Kawamura, K. Hayashi, A. Inoue, and T. Masumot, Mater. Trans. 42 (2001)1172.
[3] A. Inoue, M. Matsushita, Y. Kawamura, K. Amiya, K. Hayashi, and J. Koike, Mater. Trans. 43 (2002) 580.
[4] A. Ono, E. Abe, T. Itoi, M. Hirohashi, M. Yamasaki, and Y. Kawamura, Mater. Trans. 49 (2008)990.
[5] Y. M. Zhu, M. Weyland, A. J. Morton, K. Oh-ishi, K. Hono, and J. F. Nie, Scr. Mater. 60 (2009) 980.
[6] M. Yamasaki, K. Nyu, and Y. Kawamura, Mater. Sci. Forum 937 (2003) 419.
[7] M. Nishida and T. Yamamuro, Mater. Sci. Forum 419 (2003) 715.

[8] E. Abe, Y. Kawamura, and K. Hayashi, Acta Mater. 50 (2002) 3845.
[9] D. H. Ping and K. Hono, Philos. Mag. Let. 82 (2002) 543.
[10] M. Matsuda, S. Li, and Y. Kawanura, Mater. Sci. Eng. A 393 (2005) 269.
[11] M. Yamasaki, T Anan, and S. Yoshimoto, Scr. Mater. 53 (2005) 799.
[12] K. Amiya1, T. Ohsuna, and A. Inoue, Mater. Trans. 44 (2003) 2151.
[13] Y. Kawamura, T. K. Scri, S. Izumi, and M. Yamasaki, Scr. Mater. 55 (2006) 453.
[14] M. Matsuura and K. Konno, Mater. Trans. 47 (2006) 1264.
[15] Y. H. Deng, Chinese Phys. B 19 (2010) 017301.
[16] A. Datta and U. Ramamurty, Comp. Mater. Sci. 37 (2006) 69.
[17] M. Matsuura and M. Sakurai, J. Alloys Compd. 353 (2003) 240.
[18] C. Wolverton, Acta Mater. 49 (2001) 3129.
[19] Y. M. Zhu, A. J. Morton, M. Weyland, and J. F. Nie, Acta Mater. 58 (2010) 464.
[20] U. I. Zubov and N. P. Tretiakov, Phys. Lett. A 198 (1995) 223.
[21] B. R. Sahu, Mater. Sci. Eng. B 49 (1997) 74.
[22] H. Norbert and Y. D. Huang, Adv. Eng. Mater. 8 (2006) 235.